The current issue and full text archive of this journal is available at
www.emeraldinsight.com/0961-5539.htm

A flow solver for the Euler and Navier-Stokes equations for multi-phase flows with a stiffened gas equation of state

M. Taha Janan
Laboratoire de Turbomachines, Ecole Mohammadia d'Ingénieurs, Rabat, Morocco and
ENSET, Rabat-Instituts, Rabat, Morocco, and
A. El Marjani
Laboratoire de Turbomachines, Ecole Mohammadia d'Ingénieurs, Rabat, Morocco

Received 26 April 2005
Revised 16 June 2006
Accepted 26 July 2006

Abstract

Purpose – This paper aims to develop an efficient numerical method for simulating multicomponent flows by solving the system of conservative equations closed by a general two parameters equation of state.

Design/methodology/approach – A finite difference method for solving the two-dimensional Euler or Navier-Stokes equations for multicomponent flows in a general curvilinear coordinate system is developed. The system of conservative equations (mass, momentum and energy) is closed with a general two parameters equation of state ($\rho e = (p + \gamma p_\infty)/(\gamma - 1)$), which, associated to a γ-formulation, allows easy computation of multicomponent flows. In order to enforce the stability of the numerical scheme, the Roe's flux-difference splitting is adopted for the numerical treatment of the inviscid fluxes. The method is adapted to treat also unsteady flows by implementing an explicit Euler scheme.

Findings – The method was applied to compute various configurations of flows, ranging from incompressible to compressible fluid, including cases of single component flows or multicomponent ones**.** Computations show that the use of primitive variables instead of conservative ones, especially at low Mach numbers, improves the iteration process when the resolution is performed with a relaxation procedure such as Gauss-Seidel method. Simulations of compressible flows with a strong shock show the ability of the present method to capture shocks correctly even with the use of primitive variables. To complete numerical tests, flows involving two fluids with the presence of interactions between a shock and a discontinuity surface have been treated successfully. Also, a case of cavitating flow has been considered in this work.

Originality/value – The present method permits the simulation of a large variety of multicomponent complexes flows with an efficient numerical taking advantage of Roe's flux-difference splitting in curvilinear coordinate system.

Keywords Flow, Finite difference methods, Fluid dynamics

Paper type Research paper

1. Introduction

Modern numerical methods in computational fluid dynamics (CFD) offer a number of possibilities that allow the treatment of various flows encountered in the practice. In fact the developments of these methods during the last decades have known a great

International Journal of Numerical Methods for Heat & Fluid Flow
Vol. 17 No. 8, 2007
pp. 823-835

0961-5539
DOI 10.1108/09615530710825792

progress, thanks to the one known on computers. Nevertheless, there are still a lot of challenges among which one of the most important is to provide engineers with analysis and design tools rather than just computing tools. This can be achieved by incorporating in numerical methods, as much as possible, models that can describe practical and realistic configurations with the minimum adjusting parameters and minimum cost. In this context, we are interested in the simulation of multicomponent flows for viscous, compressible or incompressible fluids. These kinds of configurations are characterized by the presence of contact discontinuities and possible shock waves propagation. Several models that describe such situations are found in the literature. Detailed reviews are presented by Clarke *et al.* (1993) and Shyue (1998) for example. Two categories can be distinguished: front tracking methods and shock-capturing ones. We focus only on the latest category, commonly used, and adopted here in our approach. In such method, the Navier-Stokes or Euler equations are used to express the conservation of mass, momentum and energy. The numerical scheme is constructed in a way that permits to handle shocks and contact discontinuities. The presence of more than one fluid is taken into account via the adoption of a "stiffened" two parameters equation of state in a so-called gamma model. The gamma model adopted is an extension to general curvilinear coordinates of the method described by Shyue (1998) which has been derived initially by Abgrall (1994) for polytropic gases in one dimension. Each component is characterised by its ratio of specific heats γ and the mass fraction in any point of the flow that could be computed by considering an equation relating these two quantities. With the adoption of a gamma-based model, positivity of the mass fraction is preserved in opposition to the models that employ the mass fraction as a variable. In these latter methods, the determination of the mass fraction may result in negative values during iterative processes usually used and a breakdown of the computations may occur (Larrouturo, 1992). It was preferred here to use the gamma model for this reason and also to make the scheme able to compute compressible as well as incompressible fluid flows by setting properly the parameters of the equation of state. Efficient shock-capturing methods are available to solve the system generated by the mathematical model. It is well-known that for cases similar to those we are interested in, the way the inviscid fluxes are treated is crucial for the behaviour of any scheme adopted and for the accuracy of computed results. Among a great number of possibilities that are used in finite difference methods such as total variation diminishing (Harten, 1983) or essentially non oscillatory (Liu *et al.*, 1994) we use a Roe's flux-difference splitting (Roe, 1981) based method. The flux-difference splitting of Roe is an approximate Riemann solver and suffers from some shortcomings that has been widely discussed by Quirk (1994), but offers possibilities for treating shocks and contact discontinuities that have been proven in several works. We also point out that we use the grid aligned approach, that is, the direction of upwinding is set normal to the grid lines. Special attention is paid to the behaviour of the method at low-Mach numbers used alternatively for incompressible flows. The presence of regions with low speed for compressible fluids cases, such as in recirculating or attached flows affect the convergence rate of the solution procedure. This behaviour is due to the stiffness of the system of hyperbolic equations as the Mach number becomes very low. There are many methods for dealing with this situation. These methods use very often preconditioning techniques (Turkel, 1987; Choi and Merkle, 1993; Merkle and Choi, 1987). An alternate way to treat low-Mach number cases is the use of

primitive variables (Chen and Pletcher, 1991; Brenneis and Eberle, 1990). This latter approach is used in the present work and we have shown in an earlier work (Taha Janan and El Marjani, 1998) that the use of primitive variables rather than conservative ones in an implicit scheme reduces the number of iterations when the resolution is performed with a Gauss-Seidel method. In addition we note that the evaluation of the Jacobians of the viscous terms is simpler with the use of the primitive variables set.

2. Mathematical model

To describe a two-dimensional flow of a viscous fluid, we consider the Navier-Stokes equations written in a curvilinear system of coordinates. The case of an inviscid fluid is treated by dropping the viscous terms recovering hence the Euler equations. Developments are presented for two-dimensional case, the extension to 3D is straightforward and does not invoke any particular difficulty. The Navier-Stokes equations are cast into the conservative form that can be written in vector form in a system of fitted curvilinear coordinates (ξ,η) as follows:

$$\frac{1}{J}\frac{\partial \bar{q}_c}{\partial t}+\frac{\partial \bar{E}}{\partial \xi}+\frac{\partial \bar{F}}{\partial \eta}-\frac{1}{Re}\left(\frac{\partial \bar{E}_v}{\partial \xi}+\frac{\partial \bar{F}_v}{\partial \eta}\right)=0. \tag{1}$$

Where the parameter Re is the Reynolds number and J is the Jacobian of the geometric transformation from Cartesian to curvilinear coordinates. The quantity $\bar{q}_c$, representing the conservative variables, and the inviscid fluxes $\bar{E}$ and $\bar{F}$ have the following expressions:

$$\bar{q}_c=\frac{1}{J}\begin{bmatrix}\rho\\ \rho u\\ \rho v\\ \rho E_0\end{bmatrix}\quad \bar{E}=\frac{1}{J}\begin{bmatrix}\rho U\\ \rho uU+\xi_x p\\ \rho vU+\xi_y p\\ (\rho E_0+p)U\end{bmatrix}\quad \bar{F}=\frac{1}{J}\begin{bmatrix}\rho V\\ \rho uV+\eta_x p\\ \rho vV+\eta_y p\\ (\rho E_0+p)V\end{bmatrix}.$$

In these expressions ρ represents the density, u and v are the velocity components in Cartesian coordinates and p is referring to the absolute pressure. U and V are the contravariant velocity components and E_0 is the total energy. Their expressions are given by $U=\xi_x u+\xi_y v$, $V=\eta_x u+\eta_y v$ and $E_0=e+1/2(u^2+v^2)$, where e refers to the internal energy. In these expressions ξ_x, ξ_y, η_x and η_y denote the derivatives of the ξ and η coordinates with respect to the Cartesian coordinates x and y.

The viscous terms have the well-known expressions involving the metrics ξ_x, η_x, ξ_y and η_y and variable derivatives (Taha-Janan, 2001). As no special issues are considered for these terms we will not explicit nor their expressions neither the treatment adopted.

The system of equations (1) expresses the conservation of mass, momentum and energy and will be used for the computation of multicomponent flows. This system is closed in our formulation with a "stiffened" gas equation of state as follows:

$$\rho e=\frac{p+\gamma p_\infty}{\gamma-1}. \tag{2}$$

In this equation, the quantities γ and p_∞ are considered as variables and characterise each specie or component. The values of these two parameters for water and air, the

most commonly considered fluids are $\gamma = 5.5$ and $p_\infty = 442\,\text{Mpa}$ for water, and $\gamma = 1.4$ and $p_\infty = 0$ for air. Two additional equations have to be used, as shown in Shyue (1998) and Taha-Janan (2001), for the determination of the distribution of the parameters γ and p_∞ in the flow field in the so-called "gamma model". This distribution, which is computed taking into account the initial and boundary values, gives the distribution at every moment of the species in presence. The two additional equations can be expressed in the following strong conservative form:

$$\begin{aligned} \frac{1}{J}\frac{\partial}{\partial t}\left(\frac{\rho}{\gamma-1}\right)+\frac{\partial}{\partial \xi}\left(\frac{1}{J}\frac{\rho U}{\gamma-1}\right)+\frac{\partial}{\partial \eta}\left(\frac{1}{J}\frac{\rho V}{\gamma-1}\right)=0, \\ \frac{1}{J}\frac{\partial}{\partial t}\left(\frac{\rho\gamma p_\infty}{\gamma-1}\right)+\frac{\partial}{\partial \xi}\left(\frac{1}{J}\frac{\rho\gamma p_\infty U}{\gamma-1}\right)+\frac{\partial}{\partial \eta}\left(\frac{1}{J}\frac{\rho\gamma p_\infty V}{\gamma-1}\right)=0. \end{aligned} \tag{3}$$

These two equations are solved together with equations (1) to provide the aerodynamic, thermodynamic and species distribution fields. For more convenience these two systems of equations could be written as a single one as follows:

$$\frac{1}{J}\frac{\partial q_c}{\partial t}+\frac{\partial E}{\partial \xi}+\frac{\partial F}{\partial \eta}-\frac{1}{Re}\left(\frac{\partial E_v}{\partial \xi}+\frac{\partial F_v}{\partial \eta}\right)=0 \tag{4}$$

which is of the same form as system (1) but where the variable vector and the convective terms have the following expressions:

$$q_c=\frac{1}{J}\begin{bmatrix}\rho\\ \rho u\\ \rho v\\ \rho E_0\\ \rho/(\gamma-1)\\ \rho\gamma p_\infty/(\gamma-1)\end{bmatrix}\quad E=\frac{1}{J}\begin{bmatrix}\rho U\\ \rho uU+\xi_x p\\ \rho vU+\xi_y p\\ (\rho E_0+p)U\\ \rho U/(\gamma-1)\\ (\rho U\gamma p_\infty)/(\gamma-1)\end{bmatrix}\quad F=\frac{1}{J}\begin{bmatrix}\rho V\\ \rho uV+\eta_x p\\ \rho vV+\eta_y p\\ (\rho E_0+p)V\\ \rho V/(\gamma-1)\\ (\rho V\gamma p_\infty)/(\gamma-1)\end{bmatrix}.$$

It will be noted that the use of such a system allows the computation of the distribution of the species in presence in the flow field whatever is their number with always six equations for two dimensional cases and seven equations in three dimensional cases.

3. Numerical method

The system of equations (4), obtained by compacting systems (1) and (3) is to be solved to determine the flow characteristics. A finite difference scheme is derived making use of the flux-difference splitting of Roe for the inviscid fluxes. For time dependent solutions, the explicit Euler scheme is used. In the case of steady state solution we use the Euler implicit scheme for time discretisation of equations (4), leading to the following system:

$$\Delta q_c^n + \Delta t\left\{\frac{\partial \Delta E^n}{\partial \xi} + \frac{\partial \Delta F^n}{\partial \eta} - \frac{1}{Re}\left(\frac{\partial \Delta E_v^n}{\partial \xi} + \frac{\partial \Delta F_v^n}{\partial \eta}\right)\right\} = -\Delta t\left\{\frac{\partial E^n}{\partial \xi} + \frac{\partial F^n}{\partial \eta} - \frac{1}{Re}\left(\frac{\partial E_v^n}{\partial \xi} + \frac{\partial F_v^n}{\partial \eta}\right)\right\}. \tag{5}$$

In this expression $\Delta(.)^n = (.)^{n+1} - (.)^n$, where the superscript is relative to temporal steps and Δt represents the time step. This system is solved with respect to the quantity Δq_c^n.

As mentioned before, the treatment of the inviscid fluxes is crucial for the efficiency of the solution method. For this purpose, a flux difference splitting of Roe (1981) type has been implemented. Flux limiters are also used to maintain an accuracy up to third order biased in the regions of smooth gradients and a first order near discontinuities. Hence, the inviscid fluxes are approximated by numerical fluxes such as:

$$\begin{aligned} E^*_{i+1/2} = {} & \frac{1}{2}(E_i + E_{i+1}) - \frac{1}{2}\left|\tilde{\mathrm{A}}_{i+1/2}\right|(q_{i+1} - q_i) + \frac{1}{4}\Big\{(1-\kappa)\Psi^+_{i-1/2}\tilde{\mathrm{A}}^+_{i-1/2}(q_i - q_{i-1}) \\ & + (1+\kappa)\Psi^-_{i+1/2}\tilde{\mathrm{A}}^+_{i+1/2}(q_{i+1} - q_i) - (1-\kappa)\Psi^+_{i-1/2}\tilde{\mathrm{A}}^-_{i+1/2}(q_{i+1} - q_i) \\ & - (1-\kappa)\Psi^-_{i+3/2}\tilde{\mathrm{A}}^-_{i+3/2}(q_{i+2} - q_{i+1})\Big\} \end{aligned}$$

and

$$\begin{aligned} F^*_{j+1/2} = {} & \frac{1}{2}(F_j + F_{j+1}) - \frac{1}{2}\left|\tilde{\mathrm{B}}_{j+1/2}\right|(q_{j+1} - q_j) \\ & + \frac{1}{4}\Big\{(1-\kappa)\Psi^+_{j-1/2}\tilde{B}^+_{j-1/2}(q_j - q_{j-1}) \\ & + (1+\kappa)\Psi^-_{j+1/2}\tilde{\mathrm{B}}^+_{j+1/2}(q_{j+1} - q_j) \\ & - (1-\kappa)\Psi^+_{j-1/2}\tilde{B}^-_{j+1/2}(q_{j+1} - q_j) \\ & - (1-\kappa)\Psi^-_{j+3/2}\tilde{\mathrm{B}}^-_{j+3/2}(q_{j+2} - q_{j+1})\Big\}. \end{aligned} \tag{6}$$

The matrices $\tilde{A}$ and $\tilde{B}$ refer to Roe's averages in the curvilinear system of coordinates, and the indices i and j are, respectively, attached to ξ and η directions. The expressions of these matrices are given in the Appendix. The parameter Ψ is set equal to unity for smooth solutions and has the expression of a limiter in the presence of shocks or contact discontinuities. The parameter κ, permits to adjust the accuracy of the discretisation from fully second order upwind ($\kappa = -1$) up to a third order biased ($\kappa = 1/3$). It will be noted that we have dropped the c indices for the variable q for more convenience of the expression.

As mentioned before, our formulation is based on the use of primitive variables, represented by the vector $q_p = (p, u, v, T, (1/(\gamma-1)), ((\gamma p_\infty)/(\gamma-1)))^{\mathrm{T}}$ rather than the conservative ones $q_c = (\rho, \rho u, \rho v, \rho E_0, (\rho/(\gamma-1)), ((\rho\gamma p_\infty)/(\gamma-1)))^{\mathrm{T}}$. This may be achieved by applying chain rule to the increment of the conservative variables as follows:

$$\Delta q_c = \frac{\partial q_c}{\partial q_p}\Delta q_p = C\Delta q_p$$

with:

$$C = \begin{pmatrix} 1/T & 0 & 0 \\ u/T & (p+\gamma p_\infty)/T & 0 \\ v/T & 0 & (p+\gamma p_\infty)/T \\ (1/(\gamma-1))+(E_c/T) & ((p+\gamma p_\infty)/T)u & ((p+\gamma p_\infty)/T)v \\ 0 & 0 & 0 \\ 0 & 0 & 0 \end{pmatrix} \times \begin{pmatrix} -((p+\gamma p_\infty)/T^2) & -(\gamma(\gamma-1)p_\infty)/T & (\gamma-1)/T \\ -((p+\gamma p_\infty)/T^2)u & -(\gamma(\gamma-1)up_\infty)/T & ((\gamma-1)u)/T \\ -((p+\gamma p_\infty)/T^2)v & -(\gamma(\gamma-1)vp_\infty)/T & ((\gamma-1)v)/T \\ -((p+\gamma p_\infty)E_c)/T^2 & p-((\gamma(\gamma-1)p_\infty E_c)/T) & 1+((\gamma-1)/T)E_c \\ 0 & 1 & 0 \\ 0 & 0 & 1 \end{pmatrix}$$

where: $E_c = (1/2)(u^2 + v^2)$.

The resulting algebraic system obtained from previous discretisation steps is solved in our case either by an iterative Gauss-Seidel procedure or by an approximate LU factorisation to determine the quantities Δq_p^n. To achieve the solution of the resulting algebraic system after performing the discretizations and the approximate LU factorisation, this system may be written as:

$$([\mathrm{DD}] + [\mathrm{LL}])[\mathrm{DD}]^{-1}([\mathrm{DD}] + [\mathrm{UU}]\,\Delta q_p = \mathrm{RHS} \tag{7}$$

where we have grouped in the terms DD, LL and UU successively the diagonal, lower and upper nodes contributions as shown in the sketch of the molecule in Figure 1.

We will notice that the development of the two factors in the above expression does not render the original discretized equations. An error subsists, but as it acts on the Δq terms, it vanishes at vanishing Δq, i.e. as the convergence is reached. For this reason, the LU factorisation was preferred for steady state solutions while the Gauss-Seidel procedure was used for unsteady flows.

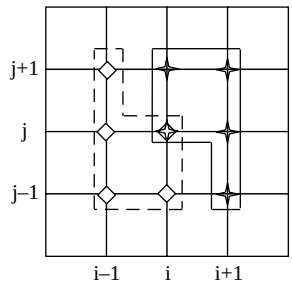

Figure 1.
Molecule used for the computation of the implicit part

The solution of the algebraic factored system is performed in two steps of, respectively, a lower and upper systems with a simple Gauss elimination.

$$\text{First step}: \quad ([DD] + [LL])\Delta q_p^* = \text{RHS}.$$

$$\text{Second step}: \quad ([DD] + [UU])\Delta q_p = [DD]\Delta q_p^*.$$

The solution q_p^{n+1} at the time step is then determined by:

$$q_p^{n+1} = q_p^n + \Delta q_p$$

The solution is then completed by updating all the other variables, especially the conservative variables used for the discretisation of the convective terms appearing in the explicit part (RHS) of the scheme.

4. Results and discussions

In order to test the numerical method described above, we have considered a variety of flows which include compressible and incompressible cases with one or more species. The results obtained for the computed configurations are described in this section.

4.1 Converging-diverging nozzle

The first test case considered is an inviscid transonic compressible flow in a converging-diverging nozzle described by Ött *et al.* (1993) and shown in Figure 2. The section of the throat represents 88 per cent of the inflow section. Computations were performed on only the half of the nozzle with symmetric conditions on the axis. A grid of 84 × 24 points, refined near the solid wall, was used. At the entry of the nozzle the total pressure and temperature were prescribed as well as a zero v component of the velocity. The value of the static pressure was fixed as a donwnstream boundary condition. The pressure along the axis of the nozzle is shown in Figure 2, which compare well to the analytic one dimensional solution. The obtained results confirm that the use of primitive variables does not affect the ability of the flux-difference splitting to capture shocks efficiently.

4.2 Constricted closed channel

The flow of an incompressible fluid in a constricted channel as described by Ghia *et al.* (1981) is computed with the present method for water by setting $\gamma = 5.5$ and

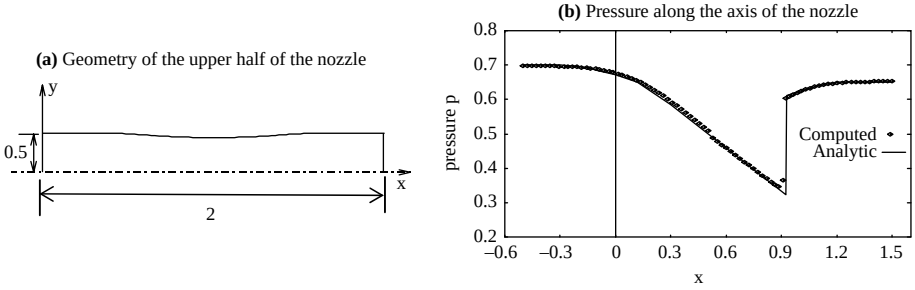

Figure 2.
Transonic nozzle

$p_\infty = 4{,}921.15$ bars. Two of the four configurations described in details by Ghia *et al.* (1981) mentioned as Cases I and II, having two different curvatures, were treated. Figure 3 shows the geometry of a constructed channel. Figure 4 shows the field of static pressure obtained for Case II, using a 21 × 61 mesh refined near the upper and lower wall, as well as in the vicinity of the region of curvature change of the channel. The inflow boundary conditions are prescribed by imposing a parabolic velocity profile, the value of the static pressure and an adiabatic condition for heat transfer. The value of the static pressure is fixed at the outflow boundary. As we deal with a viscous fluid, the velocity at the walls was set to zero, and these boundaries are considered to be adiabatic. Results show the pressure smoothness particularly in a non-staggered grid. Figure 5 shows results for wall static pressure after deducing the linear pressure profile in the case of a straight channel. We note that the results obtained by our method compare well with the ones obtained by Ghia *et al.* We should note that the stiffened gas equation of state represents well the comportment of an incompressible fluid and allows the simultaneous treatment of all the variables, including the pressure.

4.3 Richtmyer-Meshkov instability

As a test of the ability of the method developed to treat interfaces and the interaction that may occur between theses interfaces, we consider the so-called

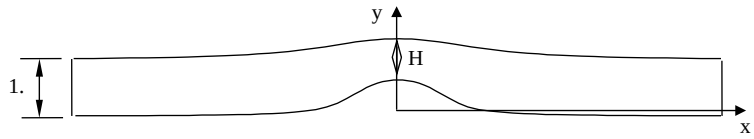

Figure 3.
Geometry of the constricted channel

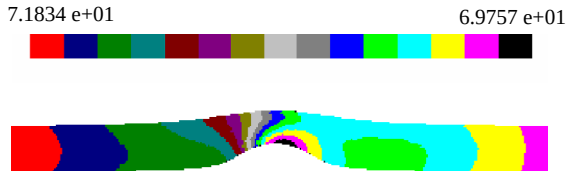

Figure 4.
Constricted channel: pressure field

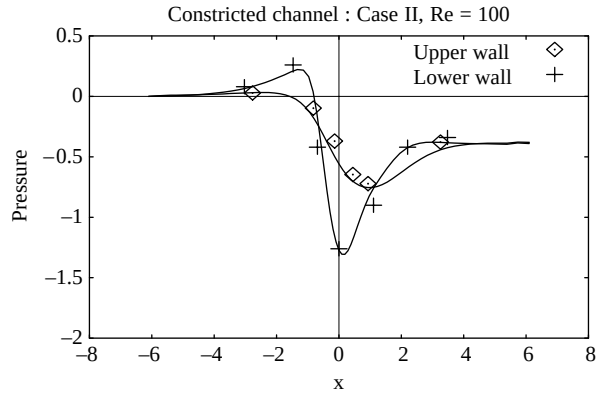

Figure 5.
Constricted channel: Static pressure at solid walls

Notes: Symbols - computational results of Ghia et al; Lines - computed results with the present method

Richtmyer-Meshkov instability. This test case deals with the interaction between a shock wave that passes an interface between two fluids with different values of acoustic impedance. The misalignment of the pressure and density gradients results in the growth of the interface perturbations and causes the development of the instability. It represents an unsteady 2D flow developed in a tube representing the interaction between a planar Mach 1.95 shock wave at $x = 1.325$ and a moving interface. The most important particularity of this case is that it involves two fluids that are, respectively, compressible and incompressible. The treatment is processed using the same equations and the same form of the equation of state for which the parameters are to be determined to follow the evolution of the interface. The initial state is represented by a gas in the left side and a liquid in the right side separated by an interface represented by:

$$x = x_0 - \varepsilon \cos(2\pi k y), \quad y \in [0, 1]$$

where $x_0 = 1.2$, $\varepsilon = 0.1$ and $k = 1$. The initial data for the left and right sides of the interface are:

$$(\rho, u, p, \gamma, p_\infty)_L = (1, 0, 1, 1.4, 0), \quad (\rho, u, p, \gamma, p_\infty)_M = (5, 0, 1, 4, 1).$$

The state behind the shock is: $(\rho, u, p, \gamma, p_\infty)_R = (7.093, -0.7288, 10, 4, 1)$.

Computations were performed on a 149×71 uniform mesh distributions, with a time step of $\Delta t = 2 \times 10^{-3}$, using Van Leer limiter. We show in Figure 6 the initial state and the density field at $t = 0.5$. As it appears in Figure 6(b), some perturbations appear for the distribution of the density. For this reason, we show in Figure 7, a comparison between the results obtained by our method for the distribution of the density at the centre line. Numerical results confirm the ability of the present method to deal efficiently with unsteady multiphase flows.

4.4 One dimensional cavitation test

We finally consider a simple introduction to simulate cavitating flows. It concerns the one dimensional flow of an incompressible flow studied earlier by Cocchi and Saurel (1997) for which the initial state is given by:

$$0 \le x < 0.5 \quad (\rho, u, v, p, \gamma, p_\infty)_L = (1., -1., 0., 0.01, 4.4, 60.)$$

$$0.5 \le x \le 1.0 \quad (\rho, u, v, p, \gamma, p_\infty)_R = (1., +1., 0., 0.01, 4.4, 60.).$$

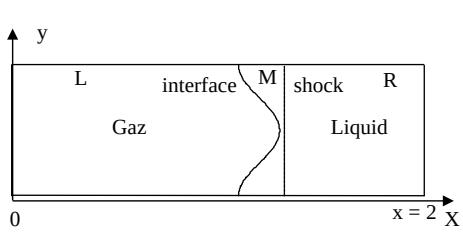

(a) Initial state

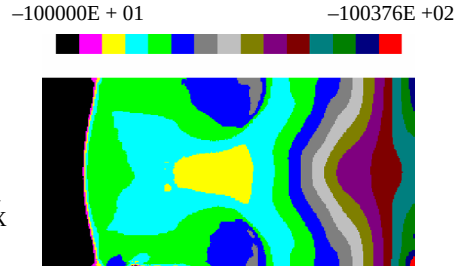

(b) Density field at t = 0.5

Figure 6.
Richtmyer-Meshkov instability

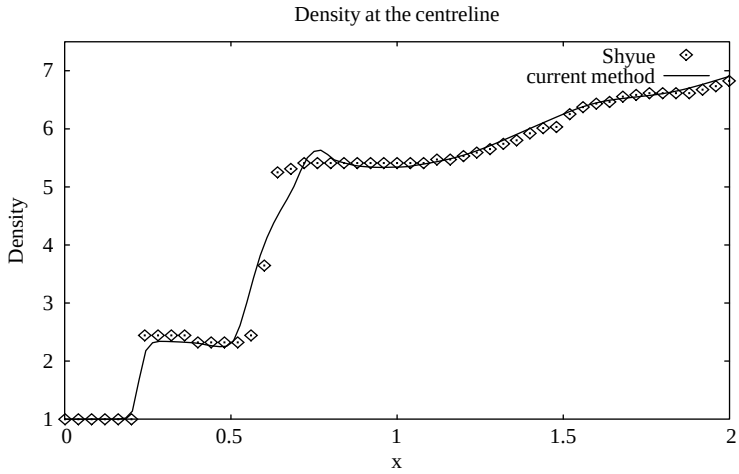

Figure 7.
Distribution of the density at the centre line

The fact that the values of the velocity are opposed in the two parts of the domain leads to the creation in the central region of highly depressed zone and then to an effect similar to the cavitation one. The cavitation criterion considered is done by imposing to the computed values of the pressure that are under the value of the saturated vapour pressure p_v, to be equal to that one. Furthermore, the density in the zones corresponding to theses values is set to be equal to the one in regions where the pressure is greater than p_v divided by 50. This value corresponds to the one generally considered in the literature. This approach permits to simulate the great differences between the densities of the two fluids.

The results obtained for this configuration, using a uniform mesh of 100 points, are shown hereafter, in Figure 8, at the time $t = 5 \times 10^{-3}$, computed with a time step of 10^{-4}. The Van Leer limiter is used.

We can observe that the computations highlight correctly the development of the depressurisation zone.

We notice that the results obtained are similar to the ones that could be obtained by a barotropic law such as the one used by Delannoy (1989). However, we are freed, here of the artifice of the connection between the two steps of constant values of the density used by Delannoy. The result related to the distribution of the density (Figure 8(c)) obtained highlights a natural connection between these two values. Furthermore, the passage of a value of the density is done on a weak extent, materializing the interface.

5. Concluding remarks

The method we developed for simulating multicomponent flows was tested for different flows configurations. The results obtained are very encouraging for further developments. The immediate applications we are working on presently are those concerning the application of the method in cavitating flows. In fact, the ability of the method to deal with multiple components as well as with discontinuities is a great trump for the application of such method in simulating cavitation which is among interesting themes in CFD. The latter presented results are very promising in that way.

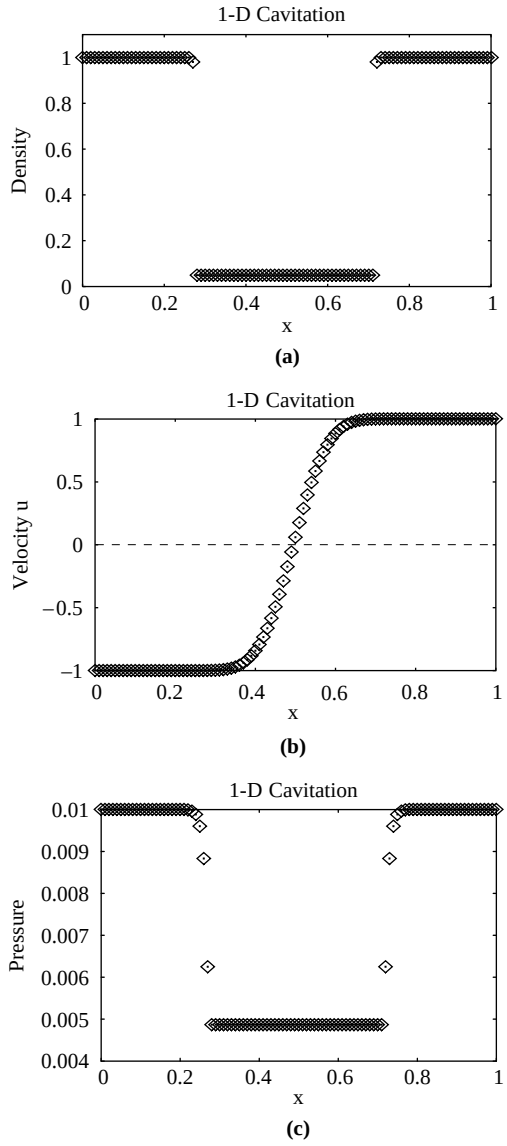

Figure 8.
(a) 1D cavitation: density distribution at = 0.005; (b) 1D cavitation: velocity distribution at $t = 0.005$; (c) 1D cavitation: pressure distribution at $t = 0.005$

References

Abgrall, R. (1994), *How to Prevent Pressure Oscillations in Multicomponent Flow Calculations: A Quasi Conservative Approach*, Rapport de recherche RR-2372, INRIA, Le Chesnay.

Brenneis, A. and Eberle, A. (1990), "Application of an implicit relaxation method solving the Euler equations for time accurate unsteady problems", *Journal of Fluid Engineering*, Vol. 112, pp. 510-20.

Chen, K-H. and Pletcher, R.H. (1991), "Primitive variable strongly implicit calculation procedure for viscous flows at all speeds", *AIAA Journal*, Vol. 29 No. 8, pp. 1241-9.

Choi, Y-H. and Merkle, C.L. (1993), "The application of preconditioning in viscous flow", *Journal of Computational Physics*, Vol. 105, pp. 207-23.

Clarke, J.F., Karni, S., Quirk, J.J., Roe, P.L., Simmonds, L.G. and Toro, E.F. (1993), "Numerical computation of two-dimensional unsteady detonantion waves in high energy solids", *Journal of Computational Physics*, Vol. 106, pp. 215-33.

Cocchi, J.P. and Saurel, R. (1997), "A Riemann problem based method for the resolution of compressible material flows", *Journal of Computational Physics*, Vol. 137, pp. 265-98.

Delannoy, Y. (1989), "Modélisation d'écoulements instationnaires et cavitants", Thèse de Doctorat, INPG, Grenoble.

Ghia, U., Ghia, K.N., Rubin, S.G. and Khosla, P.K. (1981), "Study of incompressible flow separation using primitive variables", *Computers Fluids*, Vol. 9, pp. 123-42.

Harten, A. (1983), "High resolution schemes for hyperbolic conservation laws", *Journal of Computational Physics*, Vol. 49, pp. 357-93.

Larrouturo, B. (1992), "How to preserve the mass-fractions positivity when computing compressible multi- component flows", *Journal of Computational Physics*, Vol. 95, pp. 59-84.

Liu, X-D., Osher, S. and Chang, T. (1994), "Weighted essentially non-oscillatory scheme", *Journal of Computational Physics*, Vol. 115, pp. 200-12.

Merkle, C.L. and Choi, Y-H. (1987), "Computation of low-speed flow with heat addition", *AIAA Journal*, Vol. 25 No. 6, pp. 831-8.

Ott, P., Bölcs, A. and Fransson, T.H. (1993), "Experimental and numerical study of time dependent pressure response of a shock wave oscillating in a nozzle", *ASME*, 93-GT-139.

Quirk, J.J. (1994), "A contribution to the great Riemann solver debate", *International Journal for Numerical Methods in Fluids*, Vol. 18, pp. 555-74.

Roe, P.L. (1981), "Approximate Riemann solvers, parameter vectors and difference schemes", *Journal of Computational Physics*, Vol. 43, pp. 357-72.

Shyue, K-M. (1998), "An efficient shock-capturing algorithm for compressible multicomponent problems", *Journal of Computational Physics*, Vol. 142, pp. 208-42.

Taha-Janan, M. (2001), "Contribution a la Simulation Numérique d'Ecoulements Multi-Especes pour des Fluides Compressibles ou Faiblement Compressibles", Thèse de Doctorat Es-Sciences Appliquées, Université Mohamed V, Ecole Mohammadia d'Ingénieurs, Rabat.

Taha Janan, M. and El Marjani, A. (1998), "Utilisation des Variables Primitives dans le Traitement des Ecoulements Visqueux aux Différents Nombres de Mach", *Actes de la Deuxième Conférence Internationale Sur les Mathématiques Appliquées et les Sciences de l'Ingénieur, Casablanca*, pp. 1035-40.

Turkel, E. (1987), "Preconditioning methods for solving the incompressible and low speed compressible equations", *Journal of Computational Physics*, Vol. 72, pp. 277-98.

Appendix. Expressions of Roe matrices for the model

$$\tilde{A} \text{ ou } \tilde{B} = k_1\tilde{A}_{xy} + k_2\tilde{B}_{xy}$$

for $\tilde{A}$, we set: $k_1 = Jy_\eta$ et $k_2 = -Jx_\eta$
for $\tilde{B}$, we set: $k_1 = -Jy_\xi$ et $k_2 = -Jx_\xi$

$\tilde{A}_{xy}$ and $\tilde{B}_{xy}$ are the expressions of Roe average matrices in Cartesian coordinates given by the following expressions:

$$\tilde{A}_{xy} = \begin{pmatrix} 0 & 1 & 0 & 0 & 0 & 0 \\ ((\tilde{\gamma}-3)/2)\tilde{u}^2 + ((\tilde{\gamma}-1)/2)\tilde{v}^2 & (3-\tilde{\gamma})\tilde{u} & -(\tilde{\gamma}-1)\tilde{v} & (\tilde{\gamma}-1) & \tilde{\chi} & 1-\tilde{\gamma} \\ -\tilde{u}\tilde{v} & \tilde{v} & \tilde{u} & 0 & 0 & 0 \\ ((\tilde{\gamma}-1)/2)\tilde{u}(\tilde{u}^2+\tilde{v}^2) - \tilde{u}\tilde{H} & \tilde{H} - (\tilde{\gamma}-1)\tilde{u}^2 & -(\tilde{\gamma}-1)\tilde{v}\tilde{u} & \tilde{\gamma}\tilde{u} & \tilde{\chi}\tilde{u} & (1-\tilde{\gamma})\tilde{u} \\ 0 & 0 & 0 & 0 & \tilde{u} & 0 \\ 0 & 0 & 0 & 0 & 0 & \tilde{u} \end{pmatrix}$$

and:

$$\tilde{B}_{xy} = \begin{pmatrix} 0 & 0 & 1 & 0 & 0 & 0 \\ -\tilde{u}\tilde{v} & \tilde{v} & \tilde{u} & 0 & 0 & 0 \\ ((\tilde{\gamma}-1)/2)\tilde{u}^2 + ((\tilde{\gamma}-3)/2)\tilde{v}^2 & -(\tilde{\gamma}-1)\tilde{u} & (3-\tilde{\gamma})\tilde{v} & (\tilde{\gamma}-1) & \tilde{\chi} & 1-\tilde{\gamma} \\ ((\tilde{\gamma}-1)/2)\tilde{v}(\tilde{u}^2+\tilde{v}^2) - \tilde{v}\tilde{H} & -(\tilde{\gamma}-1)\tilde{u}\tilde{v} & \tilde{H} - (\tilde{\gamma}-1)\tilde{v}^2 & \tilde{\gamma}\tilde{v} & \tilde{\chi}\tilde{v} & (1-\tilde{\gamma})\tilde{v} \\ 0 & 0 & 0 & 0 & \tilde{v} & 0 \\ 0 & 0 & 0 & 0 & 0 & \tilde{v} \end{pmatrix}$$

where the tilded variables denote the classical Roe averages.

Corresponding author
A. El Marjani can be contacted at: marjani@emi.ac.ma